

---

---

NEW TECHNOLOGIES FOR OBTAINING  
AND PROCESSING MATERIALS

---

---

## Titanium Hydroxide as a Precursor for Production of Functional Materials

L. G. Gerasimova<sup>a, \*</sup>, Yu. V. Kuzmich<sup>a, \*\*</sup>, E. S. Shchukina<sup>a, \*\*\*</sup>, and M. V. Maslova<sup>a, \*\*\*\*</sup>

<sup>a</sup> *Tananaev Institute of Chemistry and Technology of Rare Elements and Mineral Raw Materials,  
Subdivision of Kola Research Center, Russian Academy of Sciences, Apatity, Murmansk oblast, 184209 Russia*

\**e-mail: l.gerasimova@ksc.ru*

\*\**e-mail: y.kuzmich@ksc.ru*

\*\*\**e-mail: e.shchukina@ksc.ru*

\*\*\*\**e-mail: m.maslova@ksc.ru*

Received August 10, 2019; revised September 12, 2019; accepted September 13, 2019

**Abstract**—It has been found in the course of studying the phase transformations of X-ray amorphous titanium hydroxide during its mechanical activation in the presence of additives in the form of zinc compounds that finely ground powders can polymorphically transform into other nonequilibrium crystalline phases. Judging by the increase in the intensity of the peaks in the diffraction patterns, one can state that the amorphous phase crystallizes in the form of anatase and brookite as a result of high-energy exposure. It is shown that the lower the degree of hydration of titanium hydroxide, the higher the efficiency of the mechanical effect of the additive on the phase transformations. The following trend in the effect of the introduced modifier is observed:  $\text{ZnSO}_4 \cdot 7\text{H}_2\text{O} > \text{Zn}(\text{NO}_3)_2 \cdot 6\text{H}_2\text{O} > \text{ZnO}$ . This dependence is determined by the combination of physical and chemical transformations of the material located in the field of intense mechanical influence, confirmed by the calculated data on the crystallite size and microstrains. The conversion of excess mechanical energy into thermal energy initiates chemical processes resulting in the formation of solid titanium-zinc solutions that accelerate the restructuring of the crystal structure upon calcination of the modified titanium hydroxide according to the scheme anatase—brookite—rutile. The obtained results can find practical applications in the production of the so-called “rutile” nuclei used in the industrial production of multipurpose titanium dioxide.

**Keywords:** mechanical activation processing, titanium hydroxide, anatase, rutile, modifier, thermolysis, microstrains

**DOI:** 10.1134/S2075113321020155

### INTRODUCTION

Titanium dioxide, which has several structural modifications, such as anatase, rutile, and brookite, find applications in the manufacture of various products. Widespread use of titanium dioxide and especially rutile is determined by its stable structure and, accordingly, high resistance to temperature, aggressive media, and solar radiation [1]. Anatase has a metastable structure and is used in considerably smaller amounts. Brookite has not found practical applications owing to even lower technical characteristics than those of anatase. In the traditional production of titanium dioxide aimed predominantly at obtaining rutile, the modification of the titanium hydroxide (THO) precipitate that separates in the course of the thermal hydrolysis of titanium(IV) sulfate or oxychloride solution is used. The modification of titanium hydroxide accelerates the structural transformations of the material that occur during calcination [2, 3]. As a rule, the process is conducted in an aqueous titanium hydroxide suspension in the presence of modifiers. In

this case, more than one modifier is used each of which performs definite functions. The best-known modifiers that accelerate the formation of the rutile modification of titanium dioxide are compounds of zinc, aluminum, and zirconium. In addition, “rutile nuclei” are also introduced [4]. The method for producing “rutile nuclei” is rather difficult to implement; it involves the formation of a large amount of acid wastewater that requires utilization [5]. In [6], a new technique for producing zinc-containing “rutile nuclei” has been developed based on a homogeneous solid-phase process that proceeds under mechanical activation of titanium hydroxide with addition of a modifier. In the course of mechanical activation under high-energy impact on solid particles, they undergo phase transformations that cause both physical and chemical transformations in the system. Whereas the mechanical activation of titanium dioxide is discussed in numerous publications [7–9], the mechanical activation of titanium hydroxides of different degree of hydration has not received sufficient attention, espe-

**Table 1.** Objects of research

No.	Composition of the mixture prior to mechanical activation
1	Starting THO + ZnO
2	Starting THO + Zn(NO <sub>3</sub> ) <sub>2</sub> ·6H <sub>2</sub> O
3	Starting THO + ZnSO <sub>4</sub> ·7H <sub>2</sub> O
4	THO dried at 105°C + ZnO
5	THO dried at 105°C + Zn(NO <sub>3</sub> ) <sub>2</sub> ·6H <sub>2</sub> O
6	THO dried at 105°C + ZnSO <sub>4</sub> ·7H <sub>2</sub> O
7	THO dried at 250°C + ZnO
8	THO dried at 250°C + Zn(NO <sub>3</sub> ) <sub>2</sub> ·6H <sub>2</sub> O
9	THO dried at 250°C + ZnSO <sub>4</sub> ·7H <sub>2</sub> O

cially their mechanical activation in the presence of other oxides or their salts. On the other hand, the application of additives, in particular, zinc compounds, allows for the structure and activity of the processed particles to be controlled since the mechanism of action of such additives consists in increasing the concentration of point defects that facilitate the formation of solid solutions [10].

This work is aimed at the investigation of the phase transformations in the titanium hydroxide–zinc(II) solid-phase system under high-energy grinding conditions in a ball mill, which is necessary to understand the mechanisms of transformation of the surface and structural properties of the components that form the basis for physical and chemical transformations.

## EXPERIMENTAL

The main object of the study was titanium hydroxide that was precipitated by thermal hydrolysis from a binary (NH<sub>4</sub>)<sub>2</sub>TiO(SO<sub>4</sub>)<sub>2</sub>·H<sub>2</sub>O salt solution with a

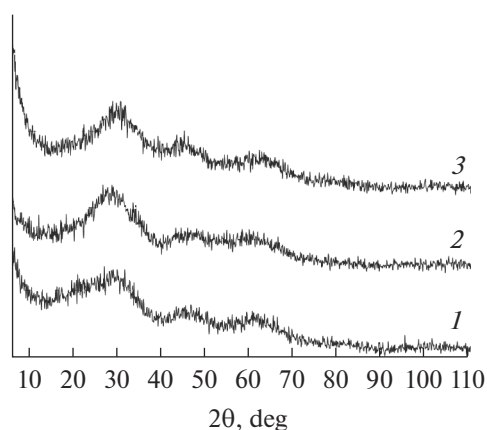


**Fig. 1.** Diffraction patterns of THO samples: (1) starting THO, (2) THO dried at 105°C, and (3) THO dried at 250°C.

concentration of TiO<sub>2</sub> of 100 g/L [11]. The resulting precipitate was thoroughly washed with water to remove the acid mother solution. The washed material was a wet powder white in color (the starting THO). Further, in the experiment, titanium hydroxide samples dried in a drying cabinet at temperatures of 105 and 250°C were used. The weight losses of titanium hydroxide upon its heat treatment were (wt %) 49.0 at 105°C and 54.1 at 250°C. Zinc oxide ZnO and Zn(NO<sub>3</sub>)<sub>2</sub>·6H<sub>2</sub>O and ZnSO<sub>4</sub>·7H<sub>2</sub>O salts were used as modifying additives. For the experiment, the test samples composed of a mixture of titanium hydroxide and zinc compounds were prepared in an agate mortar (see Table 1).

The consumption rate of the modifier was calculated as 5% ZnO of TiO<sub>2</sub> in titanium hydroxide. The mechanical activation (MA) of the resulting mixture was conducted in a Fritsch Pulverisette-7 planetary mill. The grinding jar lining and the grinding balls were made of titanium metal. The working capacity of the grinding jars was 50 mL; the weight of the grinding balls 10 mm in diameter was 60 g; the ball weight to mixture weight ratio was 10 : 1; the drum rotation speed was 750 rpm; and the treatment time was 2 h. The mechanical activation conditions were similar to those presented in previous publications on mechanical activation of solid substances, in particular, titanium dioxide [12–15]. The mechanically activated mixture was calcined at 750–850°C for 2 h.

The phase composition of the mixtures upon mechanical activation and calcination was determined using a Shimadzu XRD-6000 diffractometer.

## RESULTS AND DISCUSSION

In the traditional technology of producing titanium-containing raw materials, the titanium hydroxide to titanium dioxide conversion is performed by calcination. For targeted structuring of a hydroxide product and, accordingly, formation of titanium dioxide with desired properties, prior to calcination, a modifier is introduced into titanium hydroxide during the liquid-phase process. We have explored the possibility of a solid-phase introduction of the modifier initiating the process by mechanical activation.

X-ray diffraction analysis of the starting titanium hydroxide sample has shown its X-ray amorphous state or weak crystallinity with the anatase structure of the heat-treated samples (Fig. 1).

The influence of the temperature on the surface properties of the titanium hydroxide samples under investigation determined by nitrogen gas adsorption–desorption using a TriStar 3020 Micromeritics analyzer are provided in Table 2.

It has been noted that, with increasing temperature, the specific surface area  $S_{sp}$  of the samples decreases and, judging by a reduction in the porosity parameter  $V_{por}$ , the structure of the TiO<sub>2</sub> particles is

**Table 2.** Effect of the temperature on the surface properties of titanium hydroxide

THO samples (Fig. 1)	Processing temperature of starting THO, °C	Specific surface area $S_{sp}$ , m <sup>2</sup> /g	Total pore volume, $V_{por}$ , cm <sup>3</sup> /g	Pore diameter $D_{por}$ , nm
1	20	46.3	0.062	31.4
2	105	19.1	0.042	23.8
3	250	16.4	0.046	19.3

**Table 3.** Surface properties of THO samples upon mechanical activation

Samples upon MA	Processing temperature of starting THO, °C	Specific surface area $S_{sp}$ , m <sup>2</sup> /g	Total pore volume, $V_{por}$ , cm <sup>3</sup> /g	Pore diameter $D_{por}$ , nm
1-MA	20	42.5	0.058	29.0
2-MA	105	28.1	0.062	21.4
3-MA	250	31.3	0.066	15.1

densified, which is related to the formation of anatase crystals. The morphological evolution of powders being ground depends on their mechanical properties. The presence in the powders of water of constitution and free (surface) water influences the degree of mechanical impact of the balls on the solid particles [16]. Thus, the impact of high stresses during grinding of an X-ray amorphous powder (sample 1) is suppressed by a surface water layer on the particles. Therefore, the parameter  $S_{sp}$  hardly changes (Table 3). With the decreased intermediate water layer (heat-treated samples 2 and 3), the intensity of high-stress impact increases, which causes both mechanochemical reactions, namely, the destruction of oxo- or hydroxo-structure bridges resulting in the formation on the surface of crystal grains of the amorphous layer, and mechanophysical phenomena, namely, the formation of microdefects on the particles, which, overall, leads to an increase in the  $S_{sp}$  parameter.

High-energy mechanical impact on the titanium hydroxide–modifier mixture (Figs. 2a–2c) is accompanied by phase transformations in the samples, which is expressed in an increase in the intensity of the peak owing to the increase in the content of the anatase (A) crystalline phase and a phase similar to brookite (B). In some publications, the brookite phase is interpreted as the  $TiO_2II$  [15] or  $TiO_2-X$  phase [18]. The anatase crystallites present in starting mixtures 2 and 3 (see Table 1) serve as a seed that accelerates the crystallization process. Obviously, under mechanical activation, the physical and chemical structural transformations proceed simultaneously. The physical transformations involve the reduction in the particle size accompanied by the formation of a new active surface of the particles. In all probability, the deformation of the structure of the components of the mixture also occurs. The excess mechanical energy is converted into thermal

energy, initiating chemical processes; in particular, solid titanium–zinc solutions are formed that accelerate the restructuring with crystalline phases formed in the titanium hydroxide matrix [14]. The presence of such solid formations cannot be identified in X-ray diffraction patterns because of their small amount. It should be noted that rutile is not present in mechanically activated sample 1-MA and is observed in an insignificant quantity in some diffraction patterns of samples 2-MA and 3-MA. The transformations occur predominantly in the amorphous titanium hydroxide–anatase–brookite system, which is consistent with the data of [17, 18].

The nature of the modifier influences the structuring of titanium hydroxide under mechanical activation in the following way: It is noted that, upon mechanical activation, in diffraction patterns of the titanium hydroxide samples heat-treated in the presence of modifiers, there are practically no individual peaks that are evidence of the presence of the brookite phase. One can judge whether it is present only on the basis of split peaks that, owing to superposition, belong to both anatase and brookite. In the diffraction patterns of the mechanically activated X-ray amorphous titanium hydroxide and modifier, sufficiently distinct individual peaks of brookite are observed. According to the influence of the nature of modifiers on the efficiency of restructuring of both the starting and the heat-treated titanium hydroxide, the following trend can be suggested:  $ZnSO_4 \cdot 7H_2O > Zn(NO_3)_2 \cdot 6H_2O > ZnO$ .

The heat treatment of the mechanically activated samples was conducted at temperatures of 750, 800, and 850°C for 2 h. It was stated (Table 4) that, within the temperature variation range under investigation, there was no brookite phase in the calcined samples. Judging from the data provided, the amount of each phase depends on the nature of the zinc-containing

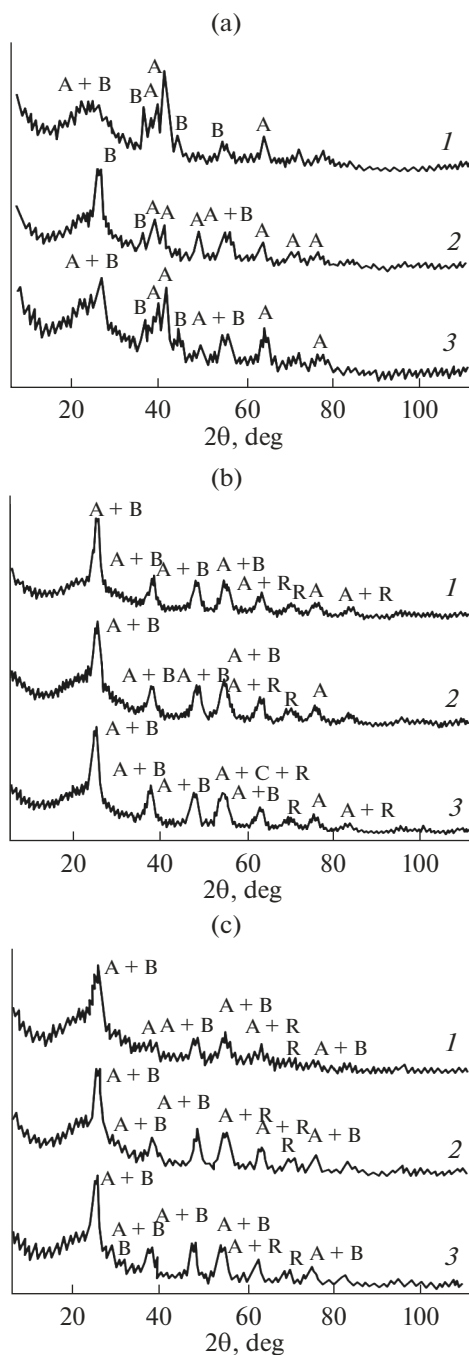


**Fig. 2.** Diffraction patterns of mixtures of titanium hydroxides with additives (a) ZnO, (b)  $Zn(NO_3)_2 \cdot 6H_2O$ , and (c)  $ZnSO_4 \cdot 7H_2O$ ; titanium hydroxide: (1) wet, (2) dried at  $105^\circ C$ , and (3) dried at  $250^\circ C$ .

additive and the calcination temperature of the samples. An increase in the temperature initiates a phase transition in the modified powders, and at  $850^\circ C$ , the rutile phase is practically completely formed.

Analysis of diffraction reflections yielded the data on the size and microstrains of the crystallites. The analysis was performed by approximating the reflec-

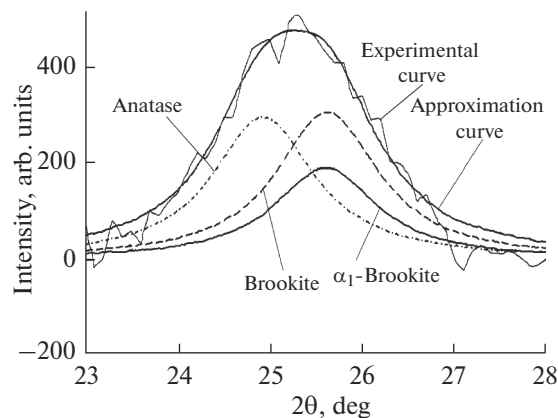


**Fig. 3.** Shapes of the reflections after their transformation using Cauchy functions.

tions using pseudo-Voigt functions (superposition of the Gaussian and Lorentzian functions) as [20–22]

$$V(\theta) = ca \left[ 1 + \frac{(\theta - \theta_0)^2}{\theta_L^2} \right]^{-1} + (1 - c)a \exp \left[ -\frac{(\theta - \theta_0)^2}{\theta_G^2} \right], \quad (1)$$

where  $c$  is the relative contribution of the Lorentzian function to the total intensity of the reflection;  $\theta_L$  and  $\theta_G$  are the Lorentzian and Gaussian distribution parameters, respectively;  $a$  is the normalizing factor of the intensity; and  $\theta_0$  is the position of the maximum of the function.

The diffraction patterns were taken in  $CuK_\alpha$  radiation and each reflection is the sum of the pulses of a doublet ( $\alpha_1, \alpha_2$ ). As a result, to describe one reflection, two pseudo-Voigt functions were used. The mutually overlapping reflections were separated using Cauchy functions. As an example, in Fig. 3, the shapes of separated anatase and brookite reflections are shown in the region  $2\theta = 25^\circ$ .

The separation of the reflections allows the calculation of the coherent scattering regions (CSRs) for individual phases. The size of the CSR and the magnitude of the microstrain of the crystallite lattice were determined by lines (210) and (321) of  $TiO_2$  (brookite) using the formula [23]

$$(\beta \cos \theta)^2 = \left( \frac{\lambda}{D} \right)^2 + (4\epsilon \sin \theta)^2, \quad (2)$$

where  $\beta$  is the physical broadening of the line of the  $\alpha_1$  reflection,  $\lambda$  is the wavelength of the copper radiation,  $D$  is the size of the CSR, and  $\epsilon$  is the magnitude of the microstrain of the crystal lattice. The obtained results are presented in Table 5.

The calculated results made it possible with a certain degree of probability to establish the trend in the changes in the found values depending on the thermal

**Table 4.** Dependence of the phase composition of the activated samples on the calcination temperature

Sample characteristic	Calculated phase composition, wt %		
	750°C	800°C	850°C
Modifier ZnO			
1	R—40; A—55; amorphous—up to 5	R—65; A—35	R—95; A—up to 5
2	R—45; A—55	R—70; A—30	R—100
3	R—50; A—55	R—73; A—27	R—100
Modifier ZnSO <sub>4</sub> ·7H <sub>2</sub> O			
1	R—55; A—45	R—90; A—10	R—100
2	R—60; A—40	R—95; A—5	R—100
3	R—65; A—35	R—95; A—5	R—100
Modifier Zn(NO <sub>3</sub> ) <sub>2</sub> ·6H <sub>2</sub> O			
1	R—45; A—55	R—70; A—30	R—100
2	R—50; A—50	R—70; A—30	R—100
3	R—55; A—45	R—75; A—25	R—100

**Table 5.** Size of the CSR and magnitude of the microstrain of the lattice

No.	Composition of the mixture for mechanochemical activation	CSR size, <i>D</i> , nm	Microstrain magnitude, $\epsilon$
1	Starting titanium hydroxide + ZnO	6	$2.7 \times 10^{-7}$
2	Starting titanium hydroxide + Zn(NO <sub>3</sub> ) <sub>2</sub> ·6H <sub>2</sub> O	8	$1.9 \times 10^{-8}$
3	Starting titanium hydroxide + ZnSO <sub>4</sub> ·7H <sub>2</sub> O	11	$8.3 \times 10^{-7}$
4	Titanium hydroxide dried at 105°C + ZnO	9	$1.2 \times 10^{-7}$
5	Titanium hydroxide dried at 105°C + Zn(NO <sub>3</sub> ) <sub>2</sub> ·6H <sub>2</sub> O	10	$5.3 \times 10^{-8}$
6	Titanium hydroxide dried at 105°C + ZnSO <sub>4</sub> ·7 H <sub>2</sub> O	10	$1.8 \times 10^{-7}$
7	Titanium hydroxide dried at 250°C + ZnO	9	$3.2 \times 10^{-7}$
8	Titanium hydroxide dried at 250°C + Zn(NO <sub>3</sub> ) <sub>2</sub> ·6H <sub>2</sub> O	10	$1.3 \times 10^{-8}$
9	Titanium hydroxide dried at 250°C + ZnSO <sub>4</sub> ·7H <sub>2</sub> O	10	$1 \times 10^{-7}$

pretreatment of the starting titanium hydroxide. In particular, the size of the crystallites, irrespective of the additive used during mechanical activation, reaches its limit when titanium hydroxide is processed at 105°C and remains approximately at the same level at 250°C (Fig. 4). The water of crystallization contained in titanium hydroxide plays in this case the role of a surface-active component that enhances the Rehbinder effect during mechanical activation. The results of calculating the magnitude of microstrains show that there are practically no microstrains.

The obtained results underlie the development of technology for production of “rutile” nuclei used in the modern technology for large-scale production of industrial titanium dioxide pigment. The newly developed technology consists of several sequential stages [24]:

(i) heat treatment of titanium hydroxide at a temperature of 110–120°C for 3h;

(ii) mixing of titanium hydroxide with a modifier, in particular, zinc sulfate, in the amount of 3.5–5% ZnO of the mass of TiO<sub>2</sub> in titanium hydroxide;

(iii) mechanical activation of the mixture in a planetary ball mill at 650–750 rpm for 2–3 h; and

(iv) addition of water to the mill up to a S : L ratio of 1 : (2–2.5) and homogenization of the mixture for 3–5 h at 500 rpm.

The fulfilment of the above conditions ensures the generation of a stable suspension with a size of the solid-phase particles of 0.3–0.5  $\mu\text{m}$  (Fig. 5), the aggregate stability of which holds for ten days.

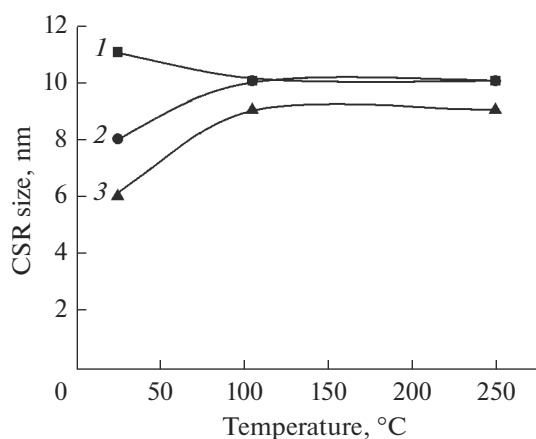


**Fig. 4.** Change in crystallite size depending on the drying temperature of the starting THO. Additives: (1)  $\text{ZnSO}_4 \cdot 7\text{H}_2\text{O}$ , (2)  $\text{Zn}(\text{NO}_3)_2 \cdot 6\text{H}_2\text{O}$ , and (3)  $\text{ZnO}$ .

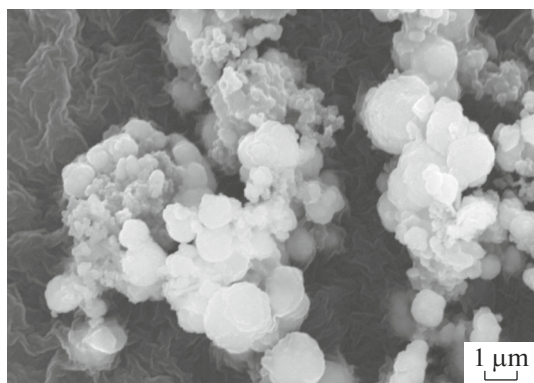


**Fig. 5.** SEM image of rutile particles in the resulting suspension of nuclei.

## CONCLUSIONS

Finely ground titanium hydroxides can polymorphically transform into other nonequilibrium crystalline phases. The study of the phase transformations of titanium hydroxide during mechanical activation with addition of  $\text{ZnO}$ ,  $\text{Zn}(\text{NO}_3)_2 \cdot 6\text{H}_2\text{O}$ , and  $\text{ZnSO}_4 \cdot 7\text{H}_2\text{O}$  has revealed that in the mixture phase transformations occur, which is expressed in an increase in the intensity of the peak owing to the increase in the content of the anatase and brookite crystalline phases. The reduction in the degree of hydration of titanium hydroxide enhances the effect of the additives on the phase transformations. The following trend in the effect of the additives has been revealed:  $\text{ZnSO}_4 \cdot 7\text{H}_2\text{O} > \text{Zn}(\text{NO}_3)_2 \cdot 6\text{H}_2\text{O} > \text{ZnO}$ . This dependence is apparently explained by the combination of the physical and chemical transformations in the material exposed to the field of an intense mechanical impact. The physical transformations contribute to the reduction in the particle size, which results in the formation of a new active surface.

The values of the microstrains and sizes of the crystallites obtained in the course of supergrinding calculated using pseudo-Voigt functions based on the analysis of the broadening of the diffraction reflections allow for a more accurate evaluation of the influence of the parameters of a ball mill on the properties of the ground powders. It has been shown that the deformation changes in the anatase crystallites have a positive effect on the phase restructuring that occurs during heat treatment; in particular, a reduction in the temperature of the anatase-to-rutile phase transition by almost  $100^\circ\text{C}$  is observed. The chemical processes, especially the formation of solid titanium-zinc solutions, initiate the conversion of excess mechanical energy into thermal energy. Further, the presence of solid solutions in the titanium hydroxide during calcination accelerates the anatase–brookite–rutile restructuring of the crystal structure.

The results obtained can find practical applications in the production of the so-called “rutile” nuclei used in the traditional industrial production of titanium dioxide. The proposed method is significantly simpler and more environmentally friendly than the established technology. Given the large scales of the production facilities in operation, the implementation of the new technology may produce a significant economic effect.

Furthermore, mechanically activated hydrated titanium dioxide powders may be of interest as such and can also serve as precursors for the preparation of classical materials the direct synthesis of which involves a number of technological and ecological drawbacks or as matrices for inclusion of required components to produce composite materials.

## REFERENCES

1. Singh, R. and Dutta, S., Synthesis and characterization of solar photoactive  $\text{TiO}_2$  nanoparticles with enhanced structural and optical properties, *Adv. Powder Technol.*, 2018, vol. 29, no. 2, pp. 211–219.
2. Ivanov, V.K., Maksimov, V.D., Shaporev, A.S., Baranchikov, A.E., Churagulov, B.P., Zvereva, I.A., and Tret'yakov, Yu.D., Hydrothermal synthesis of efficient  $\text{TiO}_2$ -based photocatalysts, *Russ. J. Inorg. Chem.*, 2010, vol. 55, no. 2, pp. 150–154.
3. Zherebtsov, D.A., Syutkin, S.A., Pervushin, V.Y., et al., Characteristics of the hydrous titanium dioxide-anatase phase transformation during hydrothermal treatment in aqueous solution, *Russ. J. Inorg. Chem.*, 2010, vol. 55, no. 8, pp. 1197–1201.
4. Viktorov, V.V., Serikov, A.S., and Belaya, E.A., Phase transformations in the  $\text{TiO}_2$ -NiO system, *Inorg. Mater.*, 2012, vol. 48, no. 5, pp. 488–493.
5. Goroshchenko, Ya.G., *Khimiya titana* (Chemistry of Titanium), Kiev: Naukova Dumka, 1970, part 2.
6. Boldyrev, V.V. and Avvakumov, E.G., Mechanochemistry of inorganic solids, *Russ. Chem. Rev.*, 1971, vol. 40, no. 10, pp. 847–859.  
<https://doi.org/10.1070/RC1971v040n10ABEH001977>

7. Delogu, F., A mechanistic study of TiO<sub>2</sub> anatase-to-rutile phase transformation under mechanical processing conditions, *J. Alloys Compd.*, 2009, vol. 468, nos. 1–2, pp. 22–27.
8. Napolitano, E., Mulas, G., Enzo, S., and Delogu, F., Kinetics of mechanically induced anatase-to-rutile phase transformations under inelastic impact conditions, *Acta Mater.*, 2010, vol. 58, no. 10, pp. 3798–3804.
9. Rezaee, M., Khoie, S.M.M., Fatmehsari, D.H., and Liu, H.K., Application of statistical methodology for the evaluation of mechanically activated phase transformation in nanocrystalline TiO<sub>2</sub>, *J. Alloys Compd.*, 2011, vol. 509, no. 36, pp. 8912–8916.
10. Boldyrev, V.V., *Ekspperimental'nye metody v mekhanokhimii tverdykh neorganicheskikh veshchestv* (Experimental Methods in Mechanochemistry of Inorganic Solids), Novosibirsk: Nauka, 1983.
11. Gerasimova, L.G., Nikolaev, A.I., Maslova, M.V., and Shchukina, E.S., Kola titanium raw material for synthesis of functional materials, *Titan*, 2016, no. 2 (52), pp. 4–11.
12. Gerasimova, L.G., Maslova, M.V., Kuzmich, Yu.V., and Shchukina, E.S., Solid-phase processes at the technology obtaining functional materials, *Fund. Issled.*, 2017, no. 1, pp. 36–43.
13. Gerasimova, L.G., Kuzmich, Yu.V., Shchukina, E.S., and Maslova, M.V., Solid-phase synthesis of titanium compounds, *Perspekt. Mater.*, 2014, no. 1, pp. 65–70.
14. Fishman, A.Ya., Ivanov, M.A., Petrova, S.A., and Zakharov, R.G., Structural phase transitions in mechanoactivated manganese oxides, *Defect Diffus. Forum*, 2010, vols. 297–301, pp. 1306–1311.
15. Sepelák, V., Bégin-Colin, S., and Le Caër, G., Transformations in oxides induced by high-energy ball-milling, *Dalton Trans.*, 2012, vol. 41, no. 39, pp. 11927–11948.
16. Bégin-Colin, S., Gadalla, A., Le Caër, G., Humbert, O., et al., On the origin of the decay of the photocatalytic activity of TiO<sub>2</sub> powders ground at high energy, *J. Phys. Chem. C*, 2009, vol. 113, no. 38, pp. 16589–16602.
17. Vorobeichik, A.I., Pryakhina, T.A., Boldyrev, V.V., et al., Mechanical activation of rutile and anatase modification of titanium dioxide and changes in their reactivity, *Izv. Sib. Otd. Akad. Nauk SSSR, Ser. Khim. Nauk*, 1983, vol. 5, no. 9, pp. 119–124.
18. Giroto, T., Bégin-Colin, S., Devaux, X., Le Caër, G., Mocellin, A., Modeling of the phase transformation induced by ball milling in anatase TiO<sub>2</sub>, *J. Mater. Synth. Process.*, 2000, vol. 8, nos. 3–4, pp. 139–144.
19. Kolesnikova, I.G., Freidin, B.M., Kuz'mich, Yu.V., and Serba, V.I., Properties of Fe-Co alloy nanopowders formed under various conditions, *Russ. Metall. (Metally)*, 2009, vol. 2009, no. 4, pp. 357–359. <https://doi.org/10.1134/S0036029509040132>
20. Kurlov, A.S. and Gusev, A.I., Effect of ball milling parameters on the particle size in nanocrystalline powders, *Tech. Phys. Lett.*, 2007, vol. 33, pp. 828–832. <https://doi.org/10.1134/S1063785007100070>
21. Belova, N.S. and Rempel, A.A., PbS nanoparticles: Synthesis and size determination by X-ray diffraction, *Inorg. Mater.*, 2004, vol. 40, no. 1, pp. 3–10.
22. Williamson, G.K. and Hall, W.H., X-ray line broadening from filed aluminium and wolfram, *Acta Metall.*, 1953, vol. 1, pp. 22–31.
23. Gerasimova, L.G., Kuzmich, Yu.V., Maslova, M.V., and Shchukina, E.S., RF Patent no. 2622302, *Byull. Izobret.*, 2017, no. 17.

*Translated by O. Lotova*